Subband structure of n-type accumulation and inversion layers in GaAs-Ge heterojunctions

J. Hautman* and L. M. Sander
Department of Physics, The University of Michigan, Ann Arbor, Michigan 48109
(Received 4 January 1985)

The density-functional method is used to calculate subband energies and densities for electrons in accumulation and inversion layers in GaAs-Ge heterojunctions. We investigate the (100), (110), and (111) orientations of the Ge surface and present our results as a function of dopant concentrations in the bulk semiconductors.

I. INTRODUCTION

The GaAs-Ge heterojunction has long been a puzzle for physicists who have been attracted by the nearly perfect match of the GaAs and Ge lattices. The uncertainty in the conduction- and valence-band discontinuities, the uncertainty over the role of Fermi-level pinning, and the apparent dependence of these properties on growth conditions are among the problems which have complicated research on this system.[1–5] In particular, these problems are unsettling for the theoretical physicist interested in details of the electronic structure. Because of the conduction-band discontinuity at the interface, we expect to see quasi-two-dimensional electron layers and subband structure analogous to that observed in the Si-SiO_2 and GaAs-$Ga_{1-x}Al_xAs$ interfaces.[6,7] While extensive calculations have been done on those systems, very little theoretical work has been attempted in the GaAs-Ge system. Merlin *et al.*[8] have used a variational method to calculate subband energy levels for an $n-$GaAs/$n-$Ge(100) heterojunction. Transitions between the single calculated subband level and the continuum were identified with observed Raman features from samples grown by molecular beam epitaxy (MBE). More recent work confirms the existence of a quasi-two-dimensional layer at this interface.[9] Some qualitatively related theoretical[10] and experimental[11] work has also been done for electron layers in the Ge(111)-insulator system. It was shown, for example, that in Ge it can be quite easy to occupy several subbands in the Ge inversion layer. This is a contrast to the Si and GaAs systems.

In spite of the uncertainties which still exist in the GaAs-Ge system, it is important to have a general idea of the kind of subband structure that can be expected in the case of an ideal heterojunction. We are also interested in seeing the importance of many-body effects in these layers. The relevant effective mass is intermediate to those of Si, where many-body effects are extremely important, and GaAs, where the effects are not very important. In this paper we calculate self-consistent subband levels and densities for electron layers on the Ge side of GaAs-Ge interfaces. The interface is assumed to be free of defect states which could pin the Fermi level. We are encouraged in this approach by the recent experimental results which suggest that defects do *not* play an important role in the GaAs-Ge heterojunction.[9,12,13] The calculations also make the approximation that the conduction-band discontinuity has a fixed value, independent of surface orientation, and we neglect any effects due to finite width of the semiconductor layers.

II. THE CALCULATIONS

The intrinsic conduction-band minimum of GaAs lies 200—300 meV above that of Ge. At an interface this discontinuity induces a transfer of electrons from the (n-type)GaAs to the Ge side where they are confined by the opposing dipole potential. The effective potential, at equilibrium, is shown in Fig. 1.

This work differs from previous calculations of this kind in that we take as input for the calculation the doping densities in the bulk on either side of the interface. For accumulation layers (n-type Ge) the relevant density of impurities in the Ge, n_{Ge}, is the acceptor concentration.[14] For inversion layers (p-type Ge) n_{Ge} is the acceptor concentration minus the donor concentration. The GaAs is assumed to be degenerate n-type with a bulk Fermi level determined by the electron concentration. The Fermi level in the Ge bulk is fixed at the appropriate impurity level. With these boundary conditions on the band-bending, the charge density in the electron layer, N_s, and in the Ge depletion layer, N_{dep}, are not independent. The structure of the subbands and the widths of the layers of fixed-space charge on both sides of the interface are all determined self-consistently as a function of the bulk

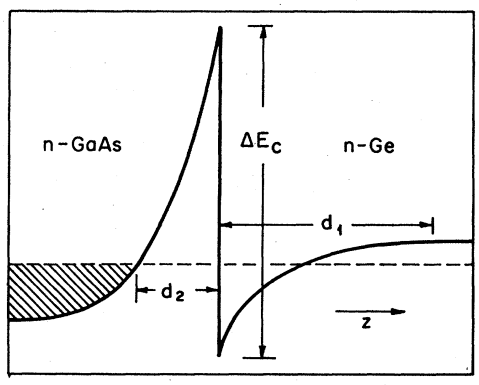

FIG. 1. Typical band-bending for an ideal GaAs-Ge heterojunction.

dopant densities. Thus, there are two distinct problems to be solved. First, the band-bending in the degenerate GaAs (the region $z \leq -d_2$ in Fig. 1) is found numerically with a Thomas-Fermi approximation.[15] This determines the slope of the electrostatic potential at the point $z=-d_2$ and hence the number of electrons, N_0, depleted from the Fermi sea. The remaining problem is the self-consistent numerical solution of the subband problem on the Ge side of the interface, along with the electrostatic band-bending and charge-conservation requirements. These requirements are incorporated into the calculation as a condition on the Ge depletion-layer width d_1 as a function of N_0 and the remaining variables N_s and $\bar{z}$, the average distance of the quasi-two-dimensional electrons from the interface. For the electrons in the Ge side we use the usual effective-mass approximation[16] and include an exchange-correlation term in the effective potential to account for many-body effects. Thus, we solve for the eigenvalues of the Kohn-Sham equations within the density-functional theory,[17] as was first done for electron layers by Ando,[18] and we assume that these energies correspond to the subband minima. We approximate the exchange-correlation potential with the usual local-density approximation.

In the effective-mass approximation the electrons are described by plane waves in the directions parallel to the interface and, in the perpendicular direction, by envelope wave functions, $\xi_i(z)$. The wave functions are solutions of the equation (all expressions are in atomic units)

$$\left[\frac{-1}{2m_z}\frac{d^2}{dz^2}+v_{\text{eff}}(z)\right]\xi_i(z)=E_i\xi_i(z) \ . \tag{1}$$

Here, m_z is the effective mass in the z direction and

$$v_{\text{eff}}(z)=v_H(z)+v_{\text{im}}(z)+v_{\text{xc}}(z) \ . \tag{2}$$

The Hartree potential $v_H(z)$ is the electrostatic potential due to the electron charge distribution, $n(z)$, and to the depletion-layer charge. The image potential,

$$v_{\text{im}}(z)=\frac{1}{4\kappa_{\text{Ge}}z}\frac{(\kappa_{\text{Ge}}-\kappa_{\text{GaAs}})}{(\kappa_{\text{Ge}}+\kappa_{\text{GaAs}})} \ , \tag{3}$$

is due to the different dielectric constants of the materials, and $v_{\text{xc}}(z)$ is the exchange-correlation potential. Starting with an initial guess for $n(z)$ and d_1 we can calculate an effective potential, solve Eq. (1), and construct a new $n(z)$. The depletion-layer width, d_1, is then determined by the band-bending requirements and the procedure is iterated to self-consistency. We have assumed a sharp interface, and make the approximation that the envelope wave functions do not leak across the interface into the GaAs. Both of these approximations have been discussed in the literature.[6,19–21] The latter is a common approximation in the Si-SiO_2 system but can be questioned in this system because of the relatively small conduction-band discontinuity. This effect has been investigated in the GaAs-$Ga_{1-x}Al_xAs$ heterojunction calculations, however, and does not seem to be very important there.[7] The GaAs-Ge interface has a comparable discontinuity and the values of m_z in Ge are larger than the value in GaAs so our results should not contain significant errors due to this simplification.

In the local-density approximation (LDA) the exchange-correlation potential $v_{\text{xc}}(z)$ is taken to be the exchange-correlation potential of a homogeneous system at the local density $n(z)$. We make the assumption that, due to the similarity of the dielectric constants of Ge and GaAs, the image potential can be neglected in the calculation of this potential. Thus, we can approximate $v_{\text{xc}}(z)$ by a simple scaling of the chemical potential of the homogeneous electron gas. In the random phase approximation (RPA) the exact scaling relationship is[22]

$$v_{\text{xc}}(z)=\frac{m_{\text{opt}}n_v}{\kappa^2}\mu(r_s^* n_v^{4/3}) \ , \tag{4}$$

where

$$r^*=\frac{m_{\text{opt}}}{\kappa}\left[\frac{3}{4\pi n(z)}\right]^{1/3} \ . \tag{5}$$

m_{opt} and κ are the optical mass and dielectric constant of Ge, and n_v is the appropriate subband valley degeneracy. In choosing to scale the potential with the optical mass, $m_{\text{opt}}=3m_t m_l/(2m_l+m_t)$, we have neglected the considerable anisotropy of the effective mass (see Table I). This approximation has been used for Ge inversion layers[10] and extensively in electron-hole liquid calculations.[23] For $\mu_{\text{xc}}(r_s)$ we use the convenient parametrized form of Gunnarsson and Lundqvist.[24] The accuracy of this parametrization has recently been improved upon[25,26] but the effect of these improvements on our results would be negligible.

An interesting complication in this approach arises on the (111) Ge surface where, in the Hartree approximation [$v_{\text{xc}}(z)=0$], we find occupation of subbands corresponding to the different sets of degenerate valleys. This problem is also relevant, in principle, for the (110) surface. In these cases, the electrons in the different sets of valleys have different exchange-correlation potentials which depend on the fraction of electrons, ζ, in that set. If we neglect intervalley exchange interaction this is analogous to the exchange-correlation potential of spins in an electron gas with arbitrary polarization. Vinter[10] has made use of this fact in extending the spin-density-functional theory[23] to calculations of ζ-dependent potentials for electrons in Ge inversion layers. Here, we obtain a potential by simple interpolation and scaling of the spin-density-functional results.

We would like to have an expression for the homogeneous exchange-correlation potential, $v_{\text{xc}}^i(r_s;\zeta)$, correspond-

TABLE I. Material parameters in atomic units (Ref. 28).

Germanium		
Dielectric constant	κ_{Ge}	16
Transverse mass	m_t	0.082
Longitudinal mass	m_l	1.59
Optical mass	m_{opt}	0.12
Gallium-arsenide		
Dielectric constant	κ_{GaAs}	13
Effective mass	m^*	0.0665

ing to each set of valleys, $i=1$, 2, as a function of ζ between 0 and 1. $v^i_{xc}(r_s;1)$ is just the chemical potential already mentioned, that other paramagnetic electron gas, scaled by the effective mass κ, and the valley degeneracy of the ith set of valleys. $v^i_{xc}(r_s;0)$ is the potential of a single minority electron. This potential corresponds to the potential of the minority spin in a ferromagnetic electron gas, $\mu^F_{xc}(r_s)$. In fact, in our approximation, which neglects intervalley exchange, both of these potentials are cases of an electron interacting with a sea of electrons via correlation interaction alone. On this basis, we make the assumption that

$$v^i_{xc}(r_s;0)\approx\frac{m_{opt}}{\kappa^2}\mu^F_{xc}(r_s^*)\ . \tag{6}$$

Ando[18] has calculated the exchange-correlation potential of an electron in the minority valleys in Si using a "Hubbard-like" approximation for the self-energy. Corresponding values of $v^i_{xc}(r_s;0)$ obtained from this minority-spin analogy are comparable. At typical densities, $r_s^*=r_s m_{opt}/\kappa=1$ and 2, we find differences of about 2% and 10% respectively. As in spin-density-functional theory we would like to interpolate between the limiting values of $v^i_{xc}(r_s;\zeta)$. This is in principle a very complicated problem, one which is not satisfactorily understood even in the spin-polarization problem.[26] In these calculations we make a linear interpolation:

$$v^i_{xc}(r_s;\zeta)=(1-\zeta)v^i_{xc}(r_s;0)+\zeta v^i_{xc}(r_s;1)\ . \tag{7}$$

We note that in the spin-density-functional case the polarization-dependent potential is very nearly linear in the polarization parameter: A linear interpolation differs from the parametrization of Gunnarsson and Lundqvist by at most 3% for values of r_s from 1 to 9.

III. RESULTS

The material parameters used are listed in Table I. For the conduction-band discontinuity we have taken $\Delta E_c=200$ meV.[27] The Fermi level was fixed at $E_f=-14.2$ meV with respect to the bulk Ge conduction band for accumulation layers, and at $E_f=-730$ meV for the inversion layers in p-type Ge.[28] All calculations are done at a temperature of 4 K: We take this into account only through the Fermi distribution of the subband electrons. Other relavent parameters can be found in Fig. 3—8.

Figure 2 shows an example of the effective potential and energy levels for an accumulation layer of Ge (110). Results are shown with and without the inclusion of the exchange-correlation potential. We see that exchange and correlation are very important in this case. The effective mass normal to the interface of the primed set of valleys is much smaller ($m_z=0.082$) than the unprimed set ($m_z=0.246$) and the many-body effects raise the $E_{0'}$ level above the E_1 level. These effects are also quite important for the (111) orientation, where we find that the number of subbands below the Fermi level will almost always be altered when exchange and correlation are included.

In Figs. 3—8 we summarize results for the different orientations of the Ge surfaces. Energy-level differences

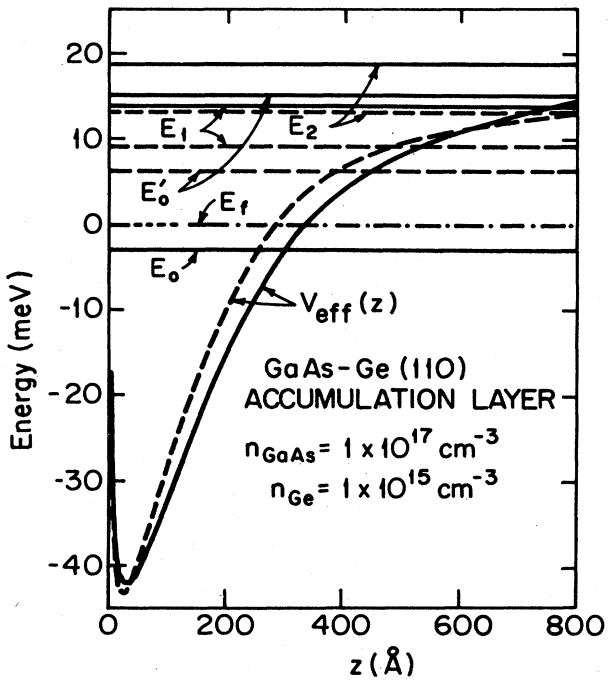

FIG. 2. Effective potential and energy levels for an accumulation layer. The dashed lines are calculated in the Hartree approximation and the solid lines are results when exchange and correlations are included. The effective potential shown is that of the lower set of degenerate valleys. E_i refers to the lower set of valley and $E_{i'}$ refers to the higher set. These doping densities correspond to $N_s=4.9\times10^{11}$ cm^{-2} and $N_{depl}=1.2\times10^{11}$ cm^{-2}. ($N_s=4.8\times10^{11}$ cm^{-2} and $N_{depl}=1.6\times10^{11}$ cm^{-2} in the Hartree case.)

are plotted as a function of doping densities in the GaAs. These results are calculated for a low density, $n_{Ge}=1\times10^{15}$ cm^{-3}. In the inversion-layer case this leads to a depletion-layer density per unit area which is fixed, to within 1% at the value.

$$N_{depl}\sim(-\epsilon_F\kappa n_{Ge}/2\pi)^{1/2}\sim1.14\times10^{11}\ \text{cm}^{-2}\ . \tag{8}$$

For the accumulation layers the value of N_{depl} varied over an order of magnitude for the range of GaAs densities considered.

The results for the (100) accumulation layer are consistent with the results of Merlin *et al.*; the many-body effects are not very important in the case where there is only a single subband. The energy levels for the (111) accumulation layer are very similar to the levels calculated by Vinter in the Ge-insulator case (using $N_{depl}=2.5\times10^{10}$ cm^{-2}), with differences attributable to the different image potentials and depletion-layer densities. More than one subband can be occupied in both the (111) inversion and (111) accumulation layers. The exchange-correlation have, however, lifted the energy levels of the higher set of valleys above the Fermi level. Overall we see a greater variety of structure than is seen in either the Si or the GaAs systems.

The effect of different Ge impurity densities was only briefly investigated. At this low concentration the effect

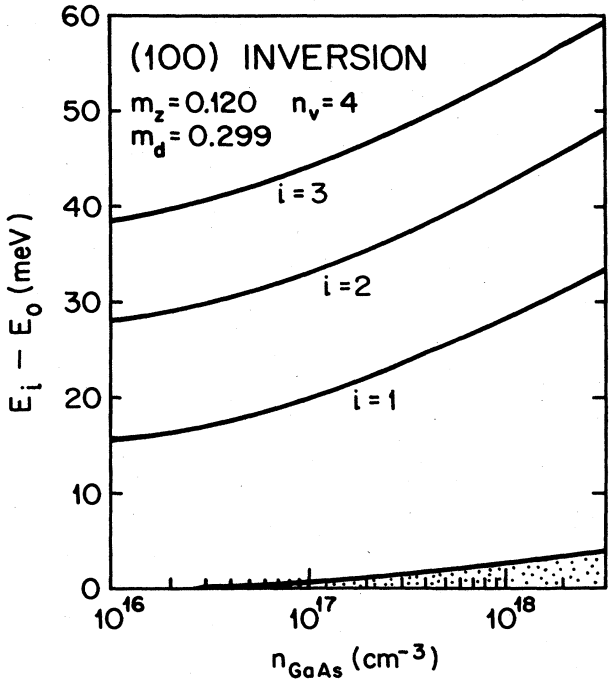

FIG. 3. Energies of some of the lowest-lying subband minima measured from the bottom of the lowest subband. The Fermi level is the line bounding the shaded region at the bottom of the figure. Results are plotted as a function of the doping in the bulk GaAs, and the doping density in the Ge is set at 1×10^{15} cm^{-3}.

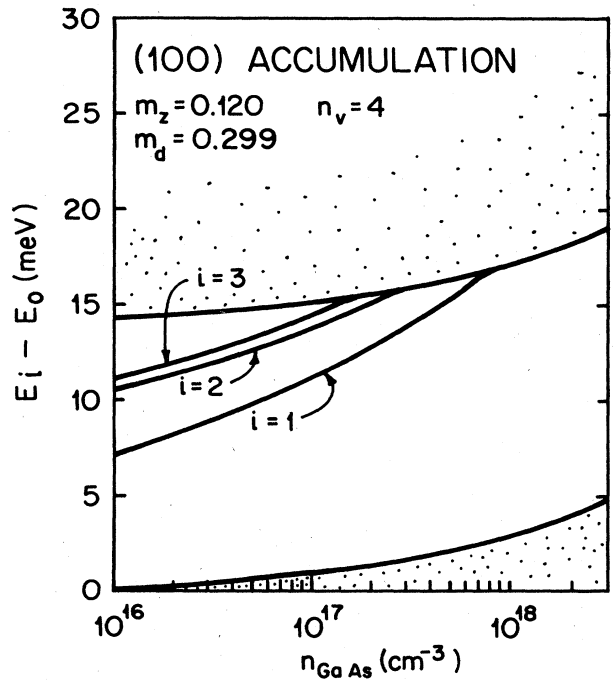

FIG. 4. Subband energy levels as in Fig. 3 except that the bulk conduction-band minimum, E_c, is included. Also note the different scale.

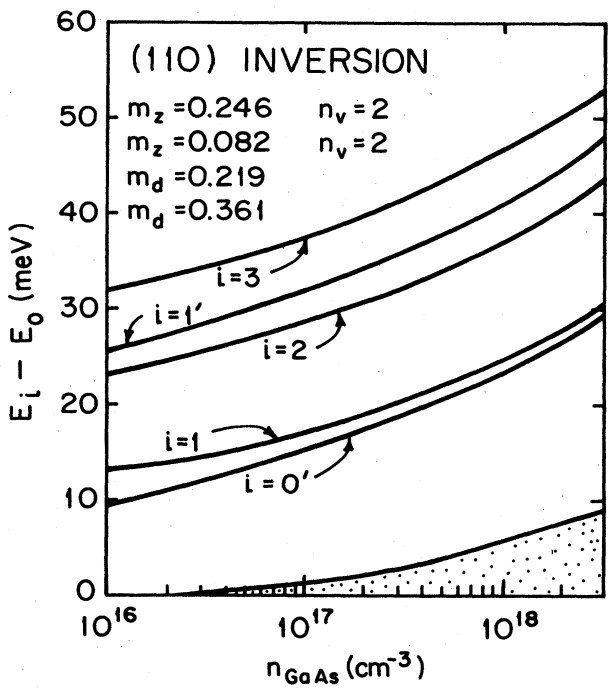

FIG. 5. Subband energy levels as in Fig. 3. The primed values of i are levels corresponding to the higher set of degenerate valleys.

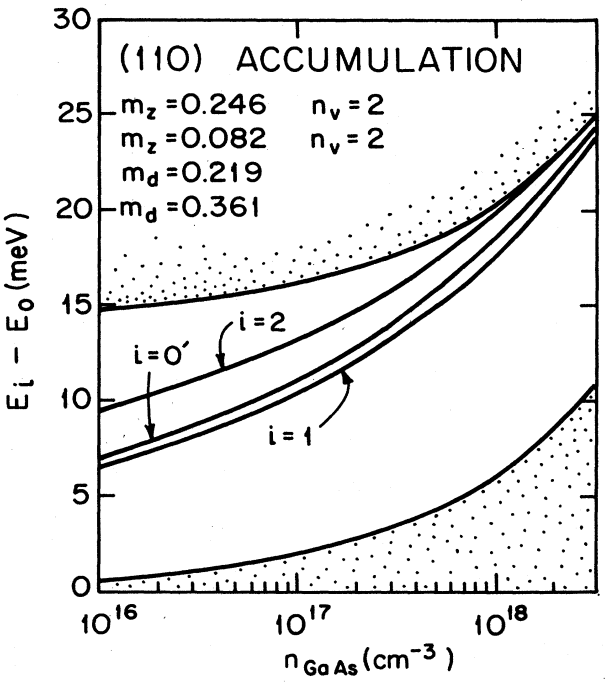

FIG. 6. Subband energy levels as in Figs. 3–5.

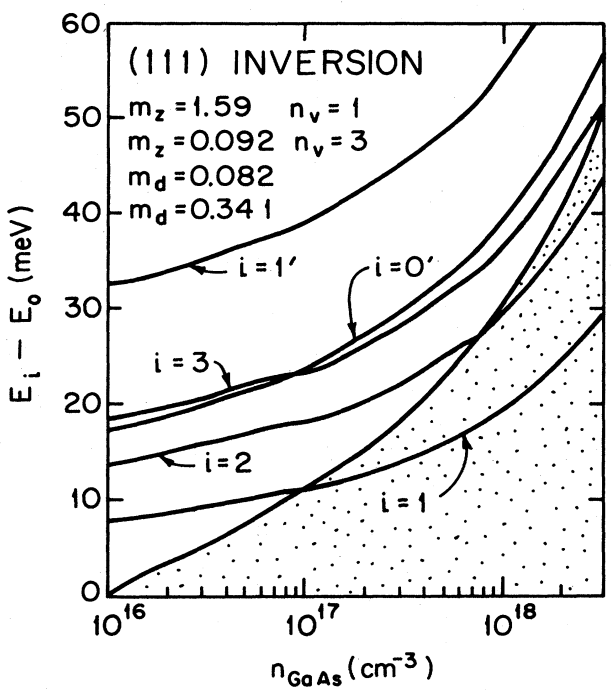

FIG. 7. Subband energy levels as in Figs. 3—6.

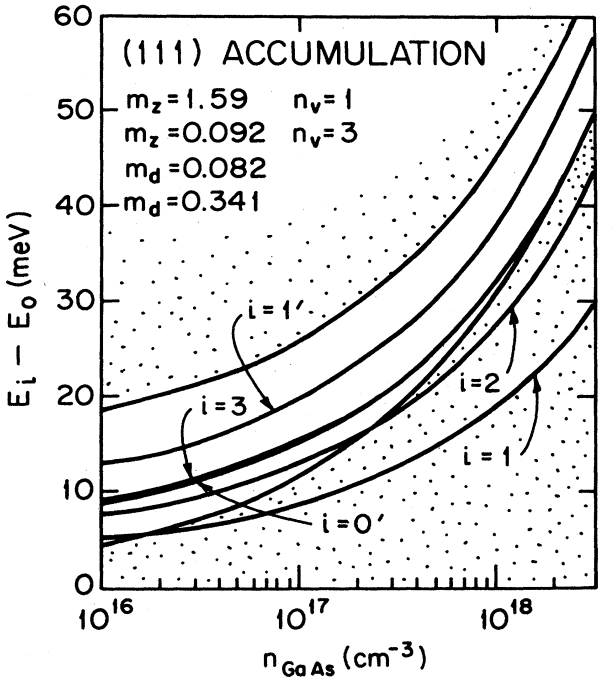

FIG. 8. Subband energy levels as in Figs. 3—7. At low densities the $E_{0'}$ level lies slightly below the E_1 level and at higher densities the order is reversed. Note that the scale here is the same as in Fig. 7.

on the layer density N_s is negligible, however, in cases where N_{depl} is on the order of, or greater than, N_s there is a significant effect on the energy-level differences (as could be expected). Selected values of N_s and N_{depl} are listed in Table II. Note that the total charge transfer $(N_s + N_{\text{depl}})$ is very closely tied to the GaAs doping concentration. Our approximation of an infinitely wide layer of Ge should be good when the width of the actual layer is on the order of, or greater than, the self-consistent depletion-layer widths. The widths corresponding to the values of N_{depl} listed in Table II range from about 10^4 Å for the inversion layers to 148—1600 Å for the accumulation layers.

Recent study indicated that ΔE_c for this interface may be closer to 300 meV rather then the value 200 meV used in these calculations.[12,29] The major effect of an increase in ΔE_c is to increase the electron-layer density. For the higher value of the ΔE_c the values of N_s are typically increased by about 20%. Since there is an approximate relationship, $N_s \propto (n_{\text{GaAs}})^{2/3}$, this would correspond to a shift of the density axes in Figs. 3—8 toward higher values [a shift of about 0.3 in $\log_{10}(n_{\text{GaAs}})$].

IV. CONCLUSIONS

Our results show the ideal GaAs-Ge system to be a very interesting system for the study of quasi-two-dimensional electron layers. The properties of these systems can be varied considerably by varying the Ge surface orientation and the Ge and GaAs doping densities. Two-dimensional charge densities as high as 3×10^{12} electrons/cm^2 were ob-

TABLE II. Values of the quasi-two-dimensional electron density N_s and the Ge depletion-layer charge density N_{depl} for different GaAs doping densities. The density of impurities in the Ge is 1×10^{15} cm^{-3}.

	Accumulation			Inversion		
n_{GaAs} (cm^{-3})	(100)	(110)	(111)	(100)	(110)	(111)
			N_s (10^{12} cm^{-2})			
10^{16}	0.148	0.150	0.151	0.0469	0.0492	0.0532
10^{17}	0.481	0.492	0.501	0.377	0.389	0.402
10^{18}	1.47	1.52	1.57	1.35	1.42	1.47
			N_{depl} (10^{12} cm^{-2})			
10^{16}	0.0166	0.0146	0.0158	0.115	0.115	0.114
10^{17}	0.0118	0.0123	0.0159	0.114	0.114	0.114
10^{18}	0.0015	0.0088	0.0160	0.114	0.114	0.114

tained with GaAs doping densities on the order of 3×10^{18} cm^{-3}. Many-body effects are shown to be important in most cases and particularly for the (110) and (111) Ge surfaces. These effects are not as large as those seen in the Si systems; however, they are very important in determining the subband structure.

The narrowness of the electron layers typically found in these and other interfaces has led the authors to question the use of the LDA in those systems.[30,31] No nonlocal calculation has been done in this case, but our estimates suggest errors, arising from nonlocal effects, on the order of 1 meV in the GaAs-Ge energy-level differences. Neglect of the problems mentioned in the Introduction may not be realistic for present samples. Observation of the subband structure discussed here may thus have to wait for more well-characterized GaAs-Ge interfaces.

ACKNOWLEDGMENTS

The authors would like to thank R. Merlin for motivating this work and for useful discussions. This work was supported by ARO Grant No. DAAG-29-83-K-0131, and NSF Grant No. DMR 82-03698.

*Present address: School of Physics and Astronomy, University of Minnesota, Minneapolis, MN 55455.

[1]G. Margaritondo, Surf. Sci. **132**, 469 (1983); R. S. Bauer and H. W. Sang, Jr., *ibid.* **132**, 479 (1983); Ping Chen, D. Bolmont, and C. A. Sibenne, *ibid.* **132**, 505 (1983); J. R. Waldrop, E. A. Kraut, S. P. Kowalczyk, and R. W. Grant, *ibid.* **132**, 513 (1983); H. Kroemer, *ibid.* **132**, 543 (1983).

[2]G. Baraff, Joel A. Appelbaum, and D. R. Hamann, Phys. Rev. Lett. **38**, 237 (1977).

[3]W. E. Pickett, S. G. Louie, and M. L. Cohen, Phys. Rev. B **17**, 815 (1978).

[4]P. Kruger and J. Pollmann, J. Vac. Sci. Technol. **B2**, 415 (1984).

[5]W. Monch, R. S. Bauer, H. Gant, and R. Murschall, J. Vac. Soc. Technol. **21**, 498 (1982).

[6]See T. Ando, A. B. Fowler, and F. Stern, Rev. Mod. Phys. **54**, 437 (1982), and references therein.

[7]T. Ando, J. Phys. Soc. Jpn. **51**, 3893 (1982).

[8]R. Merlin, A. Pinczuk, W. T. Beard, and C. E. E. Wood, J. Vac. Sci. Technol. **21**, 516 (1982).

[9]D. Gammon, R. Merlin, W. T. Beard, and C. E. E. Wood, Superlattices Microstruct. **1**, 161 (1985).

[10]B. Vinter, Phys. Rev. B **20**, 2395 (1979).

[11]J. Binder, R. Germanova, A. Huber, and F. Koch, Phys. Rev. B **20**, 2382 (1979); **20**, 2391 (1979).

[12]H. Brugger, F. Schaffler, and G. Abstreiter, Phys. Rev. Lett. **52**, 141 (1984).

[13]P. Chiaradia, A. D. Katnani, H. W. Sang, Jr., and R. S. Bauer, Phys. Rev. Lett. **52**, 1246 (1984).

[14]F. Stern, Phys. Rev. Lett. **33**, 960 (1974).

[15]R. Merlin in Ref. 8, and private communication.

[16]F. Stern and W. E. Howard, Phys. Rev. **163**, 816 (1967).

[17]See, for example, W. Kohn and P. Vashishta, in *Theory of the Inhomogeneous Electron Gas,* edited by S. Lundquist and N. H. March (Plenum, New York, 1983), p. 79.

[18]T. Ando, Phys. Rev. B **13**, 3468 (1976).

[19]F. Stern, Solid State Commun, **21**, 163 (1977); P. J. Price and F. Stern, Surf. Sci. **132**, 577 (1983).

[20]S. R. White, G. E. Marques, and L. J. Sham, J. Vac. Sci. Technol. **21**, 544 (1982).

[21]T. Ando and S. Mori, Surf. Sci. **113**, 124 (1982).

[22]W. L. Bloss, S. C. Ying, and J. J. Quinn, Phys. Rev. B **23**, 1839 (1981).

[23]W. F. Brinkman and T. M. Rice, Phys. Rev. B **7**, 1508 (1973).

[24]O. Gunnarsson and B. I. Lundqvist, Phys. Rev. B **13**, 1274 (1976).

[25]D. M. Ceperley and B. J. Alder, Phys. Rev. Lett. **45**, 566 (1980).

[26]S. H. Vosko, L. Wilk, and M. Nusair, Can. J. Phys. **58**, 1200 (1980).

[27]E. A. Kraut, R. W. Grant, J. R. Waldrop, and S. P. Kowalczyk, Phys. Rev. Lett. **44**, 1620 (1980).

[28]*Landolt-Bornstein (New Series) Group III, 17a,* edited by O. Madelung (Springer-Verlang, New York, 1982).

[29]A. D. Katnani and G. Margaritondo, J. Appl. Phys. **5**, 2522 (1983).

[30]J. Hautman and L. M. Sander, Phys. Rev. B **30**, 7000 (1984).

[31]J. Hautman and L. M. Sander, Superlattices Microstruct. **1**, 39 (1985).